Published in final edited form as:
Biochemistry. 2006 October 3; 45(39): 12039–12049. doi:10.1021/bi060663e.

The catalytic mechanism of *Escherichia coli* endonuclease VIII:

Roles of the intercalation loop and the zinc finger

Konstantin Y. Kropachev[‡], **Dmitry O. Zharkov**[*,§], and **Arthur P. Grollman**[*,‡]

‡*Department of Pharmacological Sciences, State University of New York at Stony Brook, Stony Brook, NY 11794-8651*

§*SB RAS Institute of Chemical Biology and Fundamental Medicine and Novosibirsk State University, Novosibirsk 630090, Russia*

Abstract

Endonuclease VIII (Nei) excises oxidatively damaged pyrimidines from DNA and shares structural and functional homology with formamidopyrimidine-DNA glycosylase. Although the structure of *Escherichia coli* Nei is solved, the functions of many of its amino acid residues involved in catalysis and substrate specificity are not known. We constructed a series of Nei mutants that interfere with eversion of the damaged base from the helix (QLY69-71AAA, ΔQLY69-71) or perturb the conserved zinc finger (R171A, Q261A). Steady-state kinetics were measured with these mutant enzymes using substrates containing 5,6-dihydrouracil, two enantiomers of thymine glycol, 8-oxo-7,8-dihydroguanine and an abasic site positioned opposite each of the four canonical DNA bases. To some extent, all Nei mutants were deficient in processing damaged DNA, with mutations in zinc finger mutants generally having a more profound effect. Wild-type Nei showed prominent opposite-base specificity (G>C≈T>A) when the lesion was 5,6-dihydrouracil or *cis*-(5*S*,6*R*)-thymine glycol but not for other lesions tested. Mutations in the Q69-Y71 loop eliminated this effect. Only wild-type Nei and Nei-Q261A mutants could be reductively cross-linked to damaged base-containing DNA. Experiments involving trapping with $NaBH_4$ and the kinetics of DNA cleavage catalyzed by Nei-Q261A suggested that this mutant was deficient in regenerating free enzyme from the Nei-DNA covalent complex formed during the reaction. We conclude that the opposite-base specificity of Nei is primarily governed by residues in the Q69-Y71 loop and that both this loop and the zinc finger contribute significantly to the substrate specificity of Nei.

Endonuclease VIII (Nei), a bacterial enzyme with DNA *N*-glycosylase and abasic site lyase (AP[1] lyase) activities, participates in base excision repair of oxidatively generated DNA damage (1,2). Nei is homologous to another prokaryotic enzyme, formamidopyrimidine-DNA glycosylase (Fpg) (3); together with Fpg and several eukaryotic homologs, it forms the Fpg/Nei family of DNA repair glycosylases (4,5). Despite the structural homology, Nei preferentially removes oxidatively damaged pyrimidines from substrate DNA (1,2,6), whereas Fpg excises oxidatively damaged purines (7,8). During catalysis, the Nα of the N-terminal proline moiety of Nei attacks the C1' atom of the damaged nucleoside, leading to loss of the base and formation of a Schiff base intermediate. The latter rearranges to eliminate the 3′-phosphate (β-elimination) and 5′-phosphate (δ-elimination) from the deoxyribose moiety. In bacteria, Nei likely serves as a back-up for endonuclease III, the major glycosylase with activity against oxidatively damaged pyrimidines.

[*]To whom correspondence should be addressed. D.O.Z.: tel. +7-383-335-6226, fax: +7-383-333-3677, email: dzharkov@niboch.nsc.ru. A.P.G.: tel. +1-631-444-3080, fax: +1-631-444-7641, email: apg@pharm.stonybrook.edu.

The three-dimensional structure of Nei (9) and its covalent complex with DNA (10) have been solved. Nei consists of two domains and possesses several defined structural motifs whose functional importance is evident from the structure. In particular, the enzyme everts the damaged nucleotide from DNA to gain access to C1', a target for nucleophilic attack by the N-terminal proline moiety. This eversion, referred to as "base flipping", is accompanied by the insertion of three amino acid residues (Gln-69, Leu-70 and Tyr-71, referred to here as the QLY loop or the intercalation loop) into the void left in the helix after base extrusion. The amino acids forming this short loop also participate in unstacking of the base opposite the lesion, introducing a sharp kink into DNA, and forming hydrogen bonds with the base opposite the lesion, thereby contributing to the observed opposite-base specificity.

Another important structural motif is a single C-terminal Cys_4-type zinc finger bearing an arginine residue (Arg-252), which is absolutely conserved among members of the Fpg/Nei family (11). Arg-252 is involved in a tight network of hydrogen bonds surrounding the lesion that hold DNA in a highly distorted conformation. The functions of several important residues (Pro-1, Glu-2, Glu-5, Lys-52, Asp-128, Asp-159, Glu-174, Arg-212, Arg-252) have been explored by site-directed mutagenesis (10,12). In general, mutations of amino acids involved in hydrogen-bonding at the active site compromise DNA glycosylase activity of Nei but, surprisingly, do not affect AP lyase activity. Structural studies (G. Golan, D.O. Zharkov, A.P. Grollman and G. Shoham, paper in preparation) suggest that the active site of Nei possesses sufficient flexibility to compensate for the loss of a few *prima facie* critical interactions with the abasic substrate, allowing strand scission to take place.

The substrate specificity of Nei, with regard to its preference for different lesions (lesion specificity) and for different bases opposite the lesion (opposite-base specificity), have not been systematically investigated. Approximately 20 different oxidatively damaged bases (both purine and pyrimidine derivatives) are reportedly excised by Nei (reviewed in (5)), but reports of the relative efficiency of their excision are inconsistent. The preference of Nei for the opposite base is primarily G ≥ A>(C or T) (2,13-16), although C was found to be the preferred base opposite xanthine and 8-oxo-7,8-dihydroadenine (17).

Recently, we developed a structural-bioinformatic approach designed to predict functionally important residues in DNA glycosylases (11,18). This method was used to select residues contributing to substrate specificity of Fpg, and several site-directed Fpg mutants with altered lesion or opposite-base specificity were successfully constructed (19). Here, we applied structural and conservation considerations to select residues in Nei that are likely to contribute

[1]Abbreviations :

AP apurinic/apyrimidinic

8-oxoG 2-amino-7,9-dihydro-1*H*-purine-6,8-dione (8-oxo-7,8-dihydroguanine)

DHU dihydropyrimidine-2,4(1*H*,3*H*)-dione (5,6-dihydrouracil)

F (3-hydroxytetrahydrofuran-2-yl)methyl phosphate (tetrahydrofuran analog of an abasic site)

PAGE polyacrylamide gel electrophoresis

TgA (5*S*,6*R*)-5,6-dihydroxydihydropyrimidine-2,4(1*H*,3*H*)-dione (thymine glycol enantiomer A)

TgC (5*R*,6*S*)-5,6-dihydroxydihydropyrimidine-2,4(1*H*,3*H*)-dione (thymine glycol enantiomer C).

in the multistage process of damage recognition. We report a mutational analysis of the intercalation loop and the zinc finger in Nei, and the effect of mutations in these regions on the activity and substrate specificity of this enzyme.

MATERIALS AND METHODS

Enzymes and oligonucleotides

T4 polynucleotide kinase and *E. coli* uracil-DNA glycosylase were purchased from New England Biolabs (Beverly, MA). Oligonucleotides for site-directed mutagenesis were purchased from Sigma-Aldrich (St. Louis, MO). 8-Oxo-7,8-dihydro-2′-deoxyguanosine phosphoramidite was prepared as described previously (20) and other phosphoramidites were purchased from Glen Research (Sterling, VA). Modified oligodeoxyribonucleotides for kinetic studies were synthesized by standard solid-state phosphoramidite chemistry and purified by reverse-phase high-pressure liquid chromatography. The sequence used was 5′-CTCTCCCTTCXCTCCTTTCCTCT-3′, where X was 8-oxoG, F, uracil or DHU. Duplex oligonucleotides containing a single AP site were obtained by treating the corresponding uracil-containing duplexes with uracil-DNA glycosylase according to the manufacturer's instructions; the completeness of uracil excision was confirmed by heating the product with putrescine-HCl (pH 8.0) followed by polyacrylamide gel electrophoresis (PAGE) analysis (21). Synthesis and purification of oligonucleotides containing a single thymine glycol residue were performed as described previously (22). The sequence used in this case was 5′-GACAAGCGCAGYCAGCCGAACAC-3′, where Y was (5*S*,6*R*)-Tg or (5*R*,6*S*)-Tg. The opposite strands were complementary to the corresponding modified oligonucleotides except for A, C, G or T positioned opposite the modified base. The modified strands were labeled at the 5′ position using γ-[^{32}P]ATP (Amersham Biosciences, Piscataway, NJ) and T4 polynucleotide kinase following the manufacturer's protocol, and annealed to the complementary strand in a 1:2 ratio.

Construction and purification of specific Nei mutants

Conservation analysis of the Nei subfamily of the Fpg/Nei family of DNA glycosylases was carried out as described (18). Nei mutants were produced by site-directed mutagenesis in the expression plasmid pET-24b (Novagen) carrying the wild-type *nei* coding sequence inserted at *Nde*I-*Hin*dIII restriction sites (23). The recombinant plasmids were maintained in XL1-Blue *E. coli* cells. To obtain mutant Nei proteins, the plasmids were transfected into BL21(DE3) *E. coli*. The protocol for purification of the wild-type enzyme was followed (23). No significant difference in expression or chromatographic behavior was observed between wild-type Nei and most of the mutants, with the exception of the Q261A mutant, which required 2 h (rather than 3 h) of IPTG induction and 100 mM (rather than 150 mM) NaCl in the binding buffer for chromatographic steps. Total protein concentration was determined by Bradford staining (24). To calculate the concentration of the active protein, binding of Nei to F-containing DNA was measured by the gel mobility shift assay, as described in the next section, with saturating amounts of the ligand.

Determination of apparent dissociation constants by gel mobility shift assay

Reaction mixtures contained 0.1-10 nM ^{32}P-labeled oligonucleotide duplex, 20 mM Tris-HCl (pH 7.5), 100 mM NaCl, 2 mM ethylenediamine tetraacetic acid, 1 mM dithiothreitol, 10% glycerol, and varying amounts of enzyme in a total volume of 10 μl. The enzyme was diluted with 5× reaction buffer containing 0.5 mg/ml bovine serum albumin. Reaction mixtures were pre-equilibrated at 4°C and all operations were performed at this temperature. The enzyme was added to the reaction and allowed to bind to the DNA substrate for 3 min. Aliquots (5 μl) were subjected to 8% nondenaturing PAGE (17-cm long), prerun in 0.5×TBE at 200 V for at least 2 h. Samples were loaded at 200 V, with a tracer dye (bromophenol blue, 0.5×TBE, 10%

glycerol) placed in a separate lane. Electrophoresis was continued until the dye had migrated ~6 cm from the origin. The gels were quantified using a Molecular Dynamics PhosphorImager system. Binding constants were calculated from at least three independent experiments using the nonlinear fit routine implemented in SigmaPlot v9.0 (Systat Software, Point Richmond, CA).

Assay for DNA glycosylase activities

The reaction mixture used for kinetic studies was the same as for studies of binding except that glycerol was omitted and concentrations of the labeled duplex varied accordingly to the purpose of the experiment. Reactions were initiated by addition of the enzyme and, after incubating for 0-60 min at 25°C, terminated by adding 5 μl of formamide dye and heating for 1 min at 95°C. An aliquot (5 μl) of each reaction mixture was subjected to PAGE in 20% polyacrylamide/8 M urea. Following PAGE, radioactivity levels in each band of the gel was measured on a PhosphorImager. In kinetic experiments, the enzyme concentration and length of incubation were adjusted to cleave no more than 20% of the substrate, thereby maintaining initial velocity conditions. Initial velocities (v_0) were plotted against substrate concentration $[S]_0$ and the resulting hyperbolic curves were fit to a rectangular hyperbola by least-squares nonlinear regression. Apparent values for K_M and V_{max} were obtained for the cleavage reaction; k_{cat} was calculated from the known V_{max} and the active enzyme concentration. For those cases in which we were unable to achieve saturation of substrate DNA, apparent values for the specificity constant, $k_{sp} = k_{cat}/K_M$, were obtained by linear regression of the v_0 versus $[S]_0$ plot and individual values for k_{cat} and K_M are not reported. At least three independent experiments were performed for each analysis.

Cross-linking

Reaction mixtures (10 μl) containing 20 nM of the appropriate DNA duplex, 50 nM of wild-type or mutant Nei, 25 mM Na-phosphate (pH 6.8), 50 mM NaCl, 1 mM ethylenediamine tetraacetic acid and 100 mM freshly dissolved $NaBH_4$ were incubated at 37°C for 5 min (or for the period designated in time-course experiments), quenched with 10 μl of sodium dodecyl sulfate-containing dye, heated for 5 min at 95°C, and subjected to PAGE in the Laemmli system (24). The gels were visualized using a PhosphorImager.

RESULTS

Rationale for site-directed mutagenesis

Two regions of Nei that are potentially important in determining substrate specificity and catalytic activity of the enzyme, namely, the intercalation loop and the zinc finger, have largely escaped analyses by site-directed mutagenesis (10,12). The QLY loop inserts into the space left vacant after eversion of the damaged nucleotide, forming multiple bonds with DNA. In the Fpg family, the sequence of this loop is conserved only at position 70, which is nearly always occupied by a bulky aliphatic amino acid (Leu or Met). Even more surprisingly, the exact sequence is not conserved even within the Nei subgroup; position 69 can be occupied by Gln, Gly, or a bulky residue (Fig. 1). Thus, we have constructed two mutations, one replacing all amino acids in the QLY loop with alanines (Nei-QLY/AAA) and another deleting the entire loop (Nei-ΔQLY). The first of these Nei mutants presumably retains some void-filling capabilities but loses specific side-chain interactions between the QLY loop and DNA bases; the second mutant may not be able to fill the void.

In contrast to the poorly conserved QLY loop, Arg-171 is highly conserved among Nei proteins but not in the Fpg subgroup (Fig. 1). Such subgroup-specific conservation may be indicative of residues involved in substrate specificity (11,18). This moiety lies at a distance from the lesion-binding pocket in the Nei·DNA complex and does not contact DNA directly; however,

this does not exclude it as an important determinant of specificity or catalysis as there are many examples of catalytically important residues located at a distance from the active site (25). Thus, Arg-171 was replaced with alanine (Nei-R171A). Another position, Gln-261, is absolutely conserved in Fpg and Nei (Fig. 1). As both Arg-171 and Gln-261 seem to be involved in the positioning of the zinc finger of Nei, we generated a Nei-Q261A mutant and compared its properties with those of Nei-R171A.

Binding of Nei and its mutants to damaged DNA

Many DNA glycosylases, including Nei, have a high affinity for DNA containing the tetrahydrofuran analog (F) of an AP site. Unlike natural AP sites, F is resistant to β-elimination, thus, it cannot be cleaved by DNA glycosylases with AP lyase activity. Wild-type Nei quickly processes substrates to a gapped product, while its mutants are of lower catalytic proficiency. The use of substrates containing F provides the most useful way to compare affinities of Nei and its mutants for the same lesion in DNA.

The affinities of Nei and its mutants for substrates containing F positioned opposite each of the canonical bases in DNA are listed in Table 1. The dissociation constants for wild-type proteins were similar for all pairs, with the exception of F:A, which was bound 1.5-2-fold less efficiently than other pairs. Replacement of specific side chains in the QLY loop with methyl side chains of alanine caused a ~100-fold decrease in binding efficiency but the effect of the opposite base was still negligible. However, deletion of the entire QLY loop had a dramatic effect on binding, so that F:G was bound only 2.7-fold less than the natural substrate while the K_d for F positioned opposite other bases increased ~30-60-fold. Binding of the R171A and Q261A mutants was estimated only for the F:G pair. The effect of these mutations on lesion binding was comparable to that seen with replacement or deletion of the QLY loop (Table 1).

Dissociation constants were estimated for wild-type Nei and Nei mutants binding oligonucleotides containing two known Nei substrates, *cis*-(5*S*,6*R*)-thymine glycol (Tg_A) and *cis*-(5*R*,6*S*)-thymine glycol (Tg_C). These ligands are processed by wild-type Nei, so the observed K_d reflects the wild type enzyme's affinity for both substrate and product, whereas it reflects substrate binding only for catalytically inactive Nei mutants. The values determined for Tg generally were on the same order as those for F, indicating that the affinity of Nei and its mutants for the uncleavable ligand is a good estimate of its general affinity for specific damaged DNA.

Substrate- and opposite-base specificity of wild-type Nei

To provide a basis by which to estimate the effect of mutations and to assess the specificity of Nei for different substrates under identical conditions, we determined the parameters of Michaelis-Menten kinetics for wild-type Nei acting on three well-known substrates, 5,6-dihydrouracil (DHU), Tg_A and Tg_C, as well as on 8-oxoG and AP sites. All four canonical bases were positioned opposite the lesion, except in the case of AP site when only A and G were tested as opposite bases. The results of these experiments are summarized in Table 2.

DHU often is used as a model oxidatively damaged pyrimidine substrate for Nei, endonuclease III and related enzymes (15,26). Wild-type Nei cleaved DHU efficiently when placed opposite G (Table 2), the natural context for this lesion, which is generated from C (27). A 7-9-fold decrease in the specificity constant was observed when pyrimidines were located opposite DHU, primarily due to the decrease in k_{cat}. However, when DHU was paired with A, a dramatic decrease in efficiency was observed where the DHU:A substrate was processed ~2500-fold less efficiently than DHU:G with both K_M (increasing ~20-fold) and k_{cat} (decreasing ~120-fold) contributing to this effect. A similar, albeit less dramatic pattern was observed for Tg_A: Tg_A:G was the best substrate, with Tg_A:T and Tg_A:C cleaved ~10-fold less efficiently owing

mainly to the lower k_{cat}, and Tg_A:A was the poorest substrate with the effect on K_M also being evident. Surprisingly, Nei cleaved Tg_C opposite all four bases with nearly equal efficiency, with K_M and k_{cat} being similar for these substrates (Table 2). K_M and k_{cat} values for Tg_A:A and Tg_C:A were nearly identical to measurements reported earlier on the same substrates (28), providing a control for the relative enzyme efficiency on different substrates.

As expected, wild-type Nei efficiently cleaved AP sites by β/δ elimination, with K_M decreased at least 20-fold for G opposite the lesion and up to >3 orders of magnitude for A opposite the lesion compared to substrates containing a damaged pyrimidine base (Table 2). Notably, as with Tg_C-containing substrates, no opposite-base preference of G to A was observed. The overall efficiency of AP site cleavage was 1-2 orders of magnitude higher than that of base-containing substrates, owing mainly to lower K_M values, a finding consistent with the suggestion that many DNA repair glycosylases have higher affinity for the AP product than for their base-containing substrates (29,30).

Although oxidatively damaged pyrimidines are regarded as the main substrates for Nei, several groups have reported Nei activity against 8-oxoG, a common oxidatively generated purine lesion (14,15). To analyze the effect of Nei mutations on the recognition of 8-oxoG, which may occur via a different mechanism than the one that recognizes DHU or Tg (31), we determined the kinetics of wild-type Nei on 8-oxoG-containing substrates with all four canonical DNA bases positioned opposite the lesion (Table 2). These experiments demonstrated that 8-oxoG was a much poorer substrate for wild-type Nei than was DHU or Tg, with K_M ~2 orders of magnitude less than for the oxidatively damaged pyrimidines. Together with a slight decrease in k_{cat}, this resulted in a 50- to 1,000-fold decrease in the specificity constant. No significant opposite-base effect was observed for 8-oxoG.

Activity of Nei mutants

To evaluate the contribution of the QLY loop and zinc finger to Nei catalytic activity, we measured kinetic constants for all four Nei mutants on the same set of substrates used for comparable measurements of wild-type Nei. Replacement of the QLY loop residues with alanines led to a ~2-4 orders of magnitude decrease in the enzyme's specific activity for damaged pyrimidines and 8-oxoG. The sole exception was DHU:A, where the effect was very low (2-fold) and related to the initially low specificity of wild-type Nei for this substrate. The Nei-QLY/AAA mutant showed similar k_{sp} values for DHU:A and DHU:G, the poorest and best DHU-containing substrate, respectively, for wild-type Nei. Deletion of the QLY loop rendered the enzyme completely unreactive to most DHU-containing substrates and all 8-oxoG-containing substrates. The residual activity for Tg-containing substrates was very low and was usually not saturated in steady-state kinetic experiments (Table 2). Zinc finger mutants also caused a significant reduction in catalytic activity against damaged pyrimidines and 8-oxoG. Interestingly, when the Nei-specific Arg-171 was mutated, the relative loss of activity for 8-oxoG (compared to the wild-type Nei) was 2-3 orders of magnitude less than the loss of activity for Tg. On the other hand, the Q261A mutation had a greater detrimental effect on excision of 8-oxoG than on excision of damaged pyrimidines. In both R171A and Q261A mutants, the opposite-base discrimination against A was removed, although G was still preferred as the opposite base by Nei-Q261A acting on DHU and both Tg isomers.

In our previous work (10), we showed that several mutations in key catalytic residues of Nei (Glu-2, Lys-52, Arg-252) resulted in loss of glycosylase activity but retention of the ability to cleave AP-containing DNA by β-elimination. To assess the activity of zinc finger mutants and loop mutants toward the AP site, we measured kinetic parameters for these enzymes acting on AP:A and AP:G substrates. Surprisingly, k_{cat} and K_M could be measured only for the Nei-QLY/AAA mutant; the decrease in enzyme activity due to this mutation was comparable to its effect on cleavage of base-containing substrates. Nei-R171A possessed very low but detectable

activity. As substrate saturation could not be achieved, only the k_{cat}/K_M ratio is reported (Table 2). We did not observe cleavage by Nei-Q261A and Nei-ΔQLY.

Cross-linking of Nei mutants to damaged DNA

As with other DNA glycosylases with AP lyase activity, Nei forms a transient covalent complex with DNA after base excision as well as with DNA containing abasic sites. Pro-1 attacks C1' of the damaged nucleoside to generate a Schiff base, which can be trapped by reduction with sodium borohydride or related agents. Formation of the stable trapped complex reflects the efficiency of nucleophilic attack; thus, this parameter can be used to qualitatively estimate the degree to which the enzyme's active site is perturbed by a mutation.

We investigated cross-linking of Nei and its mutants to various DNA substrates. DHU-containing substrates could be cross-linked to wild-type Nei and Nei-Q261A with no apparent opposite-base specificity, but could not be cross-linked to other Nei mutants, (Fig. 2, left column). The same held true for 8-oxoG-containing (Fig. 2, central column) and Tg-containing substrates (data not shown). On the other hand, when AP site-containing DNA was used as substrate, both WT and mutant Nei proteins demonstrated similar accumulation of the cross-linked form (Fig. 2, right column), although they showed almost no activity in cleaving this substrate (see previous section). An exception was the ΔQLY mutant, which was trapped much less efficiently (Fig. 2, right column).

Mechanism of Nei Q261A inactivation

Among the Nei mutants investigated, only the Q261A mutant could be cross-linked to damaged base-containing DNA; nevertheless, it demonstrated very low catalytic efficiency with all substrates when analyzed according to the Michaelis-Menten equation. We have assumed that the mutant form of the enzyme could form a Schiff base but could not be released from the covalent complex, resulting in low enzyme turnover. To test this hypothesis, we measured product accumulation with wild-type Nei and Nei-Q261A. Fig. 3A shows that wild-type Nei demonstrated a burst phase in the reaction of DHU:G cleavage, followed by exponential accumulation of the product up to 1 h. A burst phase also was observed for Nei-Q261A at the same concentration of the active enzyme. However, in sharp contrast to the activity of wild-type Nei, cleavage of substrate by the mutant enzyme nearly stopped after this initial reaction phase, indicating very slow product release and low enzyme turnover. The addition of more enzyme during the reaction (arrows in Fig. 3A) caused more bursts of activity, which reached the plateau as soon as the first burst, suggesting that the marked reaction slowdown is not due to exhaustion of some degraded form of the substrate that could otherwise be efficiently cleaved by Nei-Q261A.

Slow product release may result from (a) the inability of Nei to catalyze β-elimination after the Schiff base has been formed; (b) the inability of the enzyme to hydrolyze the Schiff base after β-elimination; or (c) a high affinity of the enzyme for the product in a non-covalent complex. To address these possibilities, we measured the accumulation of different forms of the Nei·DNA cross-link during treatment with $NaBH_4$. As seen in Fig. 3B, wild-type Nei formed a cross-linked complex with DHU:G within 1 min and its concentration rose steadily but slowly in 8 min, consistent with the existence of the burst phase. However, at the 15-min and 30-min time points, most of the covalent complex was converted into a higher-mobility product, likely corresponding to elimination of a cross-link with the segment of DNA 3′ to the site of covalent attachment of Nei. Nei-Q261A initially formed the complex as efficiently as did the wild-type Nei, and its concentration also increased slowly, but only a trace of the low-mobility product was observed at the longer reaction times (Fig. 3B). This result is consistent with a mechanism in which Nei-Q261A fails to initiate β-elimination after Schiff base formation.

DISCUSSION

Structural context of the mutations

The mutations studied in this paper can be divided into two groups according to their structural context. The first group, QLY69-71AAA and ΔQLY69-71, affect the tripeptide loop that the enzyme inserts into the void formed in DNA after the damaged nucleoside has been everted from the helix. This loop forms extensive contacts with DNA, including stacking, van der Waals, hydrophobic and hydrogen-bond interactions, and can be regarded as the single most important structural motif of the Nei·DNA interface, contributing 269 $Å^2$ of the total 876 $Å^2$ of the buried surface area (10). Kinetic experiments with other DNA glycosylases suggest that their void-filling elements are inserted after, rather than concurrently with nucleotide eversion, and prevent the everted lesion from falling back into the double helix (32-34). In addition, the inserted moieties often contribute to the opposite-base specificity of DNA glycosylases (35-37); in Nei, Gln-69 forms a hydrogen bond with the estranged adenine base (10). The QLY motif is not conserved in Fpg, where the residues that fill the void (Met-73, Arg-108 and Phe-110) are derived from different regions of the polypeptide. Thus, mutations of the first group are expected to destabilize the Michaelis complex and to influence the target-base and opposite-base specificity of Nei.

The second group of Nei mutations, consisting of R171A and Q261A, were predicted to affect functions of the zinc finger. Arg-171, located in the αF helix of the protein, is involved in an extensive network of hydrogen bonds spanning the tip of the zinc finger (Leu-249, Ser-250, Pro-253) and the H2TH motif (Ala-154, Asn-168). Gln-261 lies immediately C-terminal to the zinc finger, at its bottom, also interacting both with zinc finger elements (Tyr-255, Cys-257) and the remainder of the C-terminal domain (Val-172, Leu-180). Thus, Arg-171 and Gln-261 could contribute significantly to the positioning of the zinc finger during the catalytic reaction. Although Gln-261 is absolutely conserved in all members of Fpg/Nei family, Arg-171, surprisingly is not; in fact, its conservation only within the Nei subfamily was the reason it was selected for mutagenesis. In *E. coli* Fpg, Lys-154 occupies a position equivalent to that of Arg-171 in Nei but forms a different set of hydrogen bonds, possibly reflecting differences in zinc finger dynamics during substrate binding and catalysis. Interestingly, a K154A mutation in Fpg has been reported to affect both its substrate specificity and the kinetics of product release (38,39). Overall, R171A and Q261A mutations are expected to affect the substrate specificity and/or catalytic efficiency of Nei.

Substrate specificity of Nei

Initially, Nei was identified as a DNA glycosylase excising oxidatively damaged pyrimidines (1). Since then, a number of other substrates for this enzyme have been described based on limited kinetic data (5). An especially provocative finding was that Nei can remove 8-oxoG from DNA, suggesting a role for Nei as a “back-up” for Fpg (15). Importantly, this activity was reported only for oligonucleotide substrates and excision of 8-oxoG from irradiated high molecular weight DNA was not observed (6). Here, we have determined the parameters of Michaelis-Menten kinetics for wild-type Nei using several oxidatively damaged pyrimidines (DHU, Tg_A, Tg_C), 8-oxoG, and AP sites, as substrates.

In most cases (with the exception of DHU:A, see the next section) wild-type Nei excised damaged pyrimidines 2-3 orders of magnitude more efficiently than 8-oxoG. In fact, DHU:A, used as a “reference” pyrimidine lesion in a study of 8-oxoG excision by Nei (15), was the poorest of all pyrimidine substrates tested (Table 2), conveying the misleading impression that 8-oxoG is removed by Nei as efficiently as damaged pyrimidines. We conclude that 8-oxoG is *not* a physiological substrate for Nei based on (a) these kinetic data, (b) the inability of Nei to excise 8-oxoG from high molecular weight DNA (6) and (c) the insignificant difference in

G:C→T:A transversions between *fpg mutY nei* and *fpg mutY nth* triple mutants of *E. coli* (14).

DHU and both Tg enantiomers were in general efficient substrates for Nei in most opposite-base contexts. It should be noted that *cis*-Tg is subject to slow interconversion at C6 to produce *trans*-Tg even in DNA (40), and, although the majority of these lesions in our experiments were *cis*-Tg (22), a small admixture of *trans*-Tg is likely, complicating the analysis of Nei stereospecificity. Whereas Tg has been shown to appear *in vivo* during oxidative stress (41), it is not clear whether DHU is formed in the cells, as this lesion is preferentially generated by ionizing radiation under oxygen-free conditions (26), and there is no direct assay for it in biological samples. Nevertheless, DHU is widely used as a model oxidatively generated pyrimidine damage in studies on DNA repair and mutagenesis because it is an efficient substrate for DNA repair enzymes (15,42-48) and its effect on DNA polymerases is typical for oxidatively damaged pyrimidines (49,50). Therefore, use of DHU in comparison with other damaged bases may provide valuable insight into the mechanism of lesion recognition by Nei, as was done with Fpg (19).

Role of the intercalation loop in Nei catalysis and specificity

All DNA glycosylases that have been structurally investigated gain access to C1' of the lesion through eversion of the nucleotide from the DNA helix; the resulting void in the helix is occupied by amino acid residues from the protein (51). These void-filling or "plugging" residues serve several purposes. First, they stabilize the damaged nucleoside in the flipped-out conformation. Second, they form a wedge between the estranged base and those adjacent to it on the undamaged strand, thereby assisting in kinking DNA; a distortion observed in all DNA glycosylase-DNA complexes. Finally, bonds often are formed with the base opposite the lesion, contributing to opposite-base specificity.

The role of the plugging residues in catalysis have been studied for several other DNA repair glycosylases using site-directed mutagenesis. In human alkyladenine glycosylase AAG, replacement of the intercalating Tyr-162 with Ser nearly abolishes DNA binding and cleavage, whereas substituting Phe for Tyr-162 has a much less pronounced effect (52). Likewise, replacement of Arg-108 with Ala in *E. coli* Fpg reduces enzymatic activity by ~2 orders of magnitude but influences binding only minimally (19). In *E. coli* MutY, replacement of Tyr-82 by Cys leads to a decline in DNA binding, enzyme activity and its ability to complement the mutator phenotype in *mutY mutM E. coli* (53). An analogous mutation in the human MutY homolog MYH is associated with familial adenomatous polyposis (54). The replacement of Tyr-82 with Phe decreases affinity of the enzyme for damaged DNA, while Leu is a fully functional substitute for Tyr-82 (55). Perhaps the most thorough set of studies of helix plugging was performed for uracil-DNA glycosylase (Ung) from *E. coli* and humans, in which the residues involved are Leu-191 and Leu-272, respectively (33,56-58). For this enzyme, a "pinch—pull—push" model was proposed (32) in which the damaged base eversion is initiated by compression of the DNA backbone, and the Leu residue is inserted later to stabilize the flipped-out conformation. This model has been validated by stopped-flow studies for Fpg, a close relative of Nei (34,59).

In Nei, replacement of functional residues in the intercalation loop leads to a decrease of approximately 1-2 orders of magnitude in the affinity of the enzyme for damaged DNA. Deletion of this loop has an even more pronounced effect (~2-4 orders of magnitude). Thus, ~2-5 kcal/mole of the overall complex stabilization energy is provided by loop insertion, of which 0.6-3 kcal/mole is due to specific contacts made by the loop residues with DNA. The effect of loop mutations on enzyme activity is more pronounced: the specific activity of Nei-QLY/AAA is decreased ~1-4 orders of magnitude, whereas Nei-ΔQLY is completely inactive on some substrates. Interestingly, in some cases, the mutation severely affected K_M but reduced

k_{cat} to a lesser extent (e.g., 200-fold increase in K_M and a 5-fold decrease in k_{cat} for AP:G in Table 2), while in others, the opposite was observed (5-fold increase in K_M and a 1,100-fold decrease in k_{cat} for DHU:G). Destabilization of the transition state for DHU:G was approximately the same (4.2-4.3 kcal/mole, as calculated from the k_{cat} wild-type-to-mutant ratio) for both the alanine replacement and the deletion mutant, of which 3.2-3.7 kcal/mole likely results from loss of specific interactions with the DHU base (cf. ~0.5-1 kcal/mole destabilization for Tg_C:G and AP:G). Clearly, the nature of the damaged base influences events during plugging and chemistry steps even if the opposite base is the same. A similar picture was observed earlier for Fpg (19) where the R108A mutation barely affects excision of DHU:C by this enzyme (2-fold increase in k_{cat}) but more strongly inhibits excision of 8-oxoG:C (12-fold decrease in k_{cat}).

Three well-known examples of DNA glycosylases with strong opposite-base specificity are Fpg, OGG1 and MutY proteins. The first two enzymes have a strong preference for C opposite the lesion, while MutY excises A paired with G or 8-oxoG. Interestingly, even for Fpg and OGG1 the recognition of C is achieved by different structural means: in the former, a single Arg residue (Arg-108 in *E. coli* Fpg) donates hydrogen bonds to O^2 and N3 of C (36,60), whereas in OGG1, these moieties of the estranged C make bifurcated hydrogen bonds with two Arg residues, and the N^4 amine donates a hydrogen bond to an Asn side chain amide carbonyl (35). Prior to this study, Nei was not regarded as an enzyme with a pronounced opposite-base specificity, hence, the structure of Nei·DNA covalent complex was determined with A opposite the lesion (10). A single hydrogen bond formed between Nε2 of Gln-69 and N3 of A also was interpreted as a lack of opposite-base specificity. Here, however, we have shown that wild-type Nei strongly discriminates *against* A opposite the lesion, at least for some substrates (DHU and Tg_A, see Table 2). G appears to be a preferred opposite base for wild-type Nei, an observation explained by the possibility of forming an additional hydrogen bond between Oε1 of Gln-69 and N^2 of G. Elimination of this functional group in Nei-QLY/AAA and Nei-ΔQLY leads to a loss of the preference for G and discrimination against A, supporting the role of the QLY loop in determining the opposite-base specificity of Nei. Similarly, opposite-base preferences of Fpg are changed, albeit in a more complex manner, by substitution of Ala for Arg-108 (19).

Role of the zinc finger in catalysis by Nei

A single C-terminal Cys_4-type β/β-antiparallel zinc finger is a distinguishing feature of Fpg/Nei enzymes, being present in all bacterial Fpg and Nei proteins and in eukaryotic NEIL2 (5). Interestingly, even when no zinc-binding residues are apparent in the sequence alignment of eukaryotic NEIL1 proteins, this part of the protein adopts a zinc finger-like conformation ("zincless finger") in the X-ray structure of human NEIL1 (61). Disruption of the zinc finger motif by site-directed mutagenesis is detrimental for substrate binding and catalytic activity of *E. coli* Fpg (62,63). Minimal changes in the structure of this motif are tolerated; e.g., a replacement of Zn^{2+} with Co^{2+} in Fpg produces a fully active enzyme (64). In Nei, Arg-252 is positioned within a β-turn at the tip of the zinc finger where it is involved in the coordination of the phosphates flanking the lesion; mutation of this residue ablates DNA glycosylase activity but the AP lyase function is retained due to compensating structural changes in the protein-DNA complex ((10), G. Golan, D.O. Zharkov, A.P. Grollman and G. Shoham, paper in preparation). Arg-252 of Nei and the homologous Arg-258 of *E. coli* Fpg are hypothesized to play a mechanistic role in β- and δ-elimination catalyzed by these enzymes by stabilizing the negative charge at the leaving phosphate moiety (5). Obviously, a proper conformation of the zinc finger is very important for the action of Fpg/Nei enzymes. Less clear, however, is the role of the interactions between the zinc finger and the rest of the protein with respect to the specificity and activity of the enzyme.

In this paper, we investigated two Nei mutants, R171A and Q261A, that were predicted to perturb the normal positioning of the zinc finger while leaving intact the conformation of this motif. Both mutant enzymes demonstrated a pronounced loss in catalytic activity, indicating that correct interactions of the zinc finger with the remainder of the protein are important for Nei activity. Interestingly, these proteins differed with respect to their ability to cross-link to the DNA substrate after sodium borohydride treatment. While the R171A mutant was deficient in cross-linking to base-containing substrates and readily cross-linked to AP substrates, the Q261A mutant was efficiently trapped with both types of substrates, using a variety of base lesions (DHU, Tg_A, Tg_C, 8-oxoG). This observation suggests that at least the initial stage of the reaction, formation of the Schiff base is not affected by the Q261A mutation. On the other hand, certain reaction steps were markedly inhibited in this mutant. For example, product release was slow and the accumulation of different cross-linking species suggested that Nei-Q261A does not proceed to β-elimination to any significant extent. Treatment of the product with putrescine, an organic base that promotes hydrolysis of AP sites, caused a moderate increase in cleavage efficiency by Nei-Q261A but not wild-type Nei (not shown), indicating that the product in Nei-Q261A is, at least partly, an AP site, perhaps still covalently complexed to the protein as a Schiff base.

Despite the availability of the structures of free Nei (9) and Nei covalently bound to DNA (10), the precise role played by the zinc finger in the mechanism of action of Fpg/Nei enzymes is not completely clear. It has been suggested (10,36) that correct positioning of Arg-252 is crucial for base excision by Nei; however, Arg-252 has been shown to be dispensable for Schiff base formation and β-elimination at pre-formed AP sites (10). Unlike the R252A mutation, R171A and Q261A, mutations remote from the immediate DNA-binding residues, have a profound deactivating effect on substrate binding and catalysis by Nei. Analysis of the structure of free and DNA-bound Nei (9) reveals that the zinc finger changes its conformation upon DNA binding, with the tip of the finger moving ~4 Å. This leads to the loss or re-orientation of several contacts formed by Arg-171 with the zinc finger. Clearly, DNA binding requires a precise and specific motion of the zinc finger, which may be impeded in the R171A mutant. On the other hand, the changes around Gln-261 between the free and DNA-bound state are relatively minor; however, no structure of Nei is available that would reflect events occurring after Schiff base formation.

The strong inhibition of AP site cleavage by both zinc finger mutations was not expected, considering that several mutants of critical residues (Glu-2, Lys-52, Arg-252) retain good activity on this substrate. The crystal structure of Glu-2 and Arg-252 mutants bound to DNA (G. Golan, D.O. Zharkov, A.P. Grollman and G. Shoham, paper in preparation) shows that they could nevertheless adopt a conformation suitable for nucleophilic attack at a pre-formed AP site with some minor structural adjustment; thus, the machinery for lesion eversion in these mutants appears to be intact. The inactivity of Nei-R171A and Nei-Q261A on AP sites could be rationalized by defects in β-elimination, as described above, since they both efficiently cross-link to AP-DNA. The ΔQLY loop mutant, also inactive on AP sites and poorly cross-linked, is likely defective in lesion eversion due to its inability to insert the intercalation loop into the DNA helix.

In summary, we have designed and studied several mutants of Nei that proved to be defective in different stages of damaged base processing. Our results support the model of sequential recognition of the lesions (31) and underscore the importance of protein dynamics in identification and cleavage of damaged DNA by DNA repair glycosylases.

Acknowledgements

This research was supported by NIH grant CA 17395 (to A.P.G.) D.O.Z. acknowledges support from the Russian Academy of Sciences (Program 10.5), Russian Foundation for Basic Research (04-04-48253, 04-04-48254, 05-04-48619), Wellcome Trust UK (070244/Z/03/Z), and US Civilian Research & Development Foundation (Y2-B-08-08).

REFERENCES

1. Melamede RJ, Hatahet Z, Kow YW, Ide H, Wallace SS. Isolation and characterization of endonuclease VIII from Escherichia coli. Biochemistry 1994;33:1255–1264. [PubMed: 8110759]
2. Jiang D, Hatahet Z, Melamede RJ, Kow YW, Wallace SS. Characterization of *Escherichia coli* endonuclease VIII. J. Biol. Chem 1997;272:32230–32239. [PubMed: 9405426]
3. Jiang D, Hatahet Z, Blaisdell JO, Melamede RJ, Wallace SS. *Escherichia coli* endonuclease VIII: cloning, sequencing and overexpression of the *nei* structural gene and characterization of *nei* and *nei* nth mutants. J. Bacteriol 1997;179:3773–3782. [PubMed: 9171429]
4. Wallace SS, Bandaru V, Kathe SD, Bond JP. The enigma of endonuclease VIII. DNA Repair 2003;2:441–453. [PubMed: 12713806]
5. Zharkov DO, Shoham G, Grollman AP. Structural characterization of the Fpg family of DNA glycosylases. DNA Repair 2003;2:839–862. [PubMed: 12893082]
6. Dizdaroglu M, Burgess SM, Jaruga P, Hazra TK, Rodriguez H, Lloyd RS. Substrate specificity and excision kinetics of *Escherichia coli* endonuclease VIII (Nei) for modified bases in DNA damaged by free radicals. Biochemistry 2001;40:12150–12156. [PubMed: 11580290]
7. Tchou J, Bodepudi V, Shibutani S, Antoshechkin I, Miller J, Grollman AP, Johnson F. Substrate specificity of Fpg protein. Recognition and cleavage of oxidatively damaged DNA. J. Biol. Chem 1994;269:15318–15324. [PubMed: 7515054]
8. Karakaya A, Jaruga P, Bohr VA, Grollman AP, Dizdaroglu M. Kinetics of excision of purine lesions from DNA by *Escherichia coli* Fpg protein. Nucleic Acids Res 1997;25:474–479. [PubMed: 9016584]
9. Golan G, Zharkov DO, Feinberg H, Fernandes AS, Zaika EI, Kycia JH, Grollman AP, Shoham G. Structure of the uncomplexed DNA repair enzyme endonuclease VIII indicates significant interdomain flexibility. Nucleic Acids Res 2005;33:5006–5016. [PubMed: 16145054]
10. Zharkov DO, Golan G, Gilboa R, Fernandes AS, Gerchman SE, Kycia JH, Rieger RA, Grollman AP, Shoham G. Structural analysis of an *Escherichia coli* endonuclease VIII covalent reaction intermediate. EMBO J 2002;21:789–800. [PubMed: 11847126]
11. Zharkov DO, Grollman AP. Combining structural and bioinformatics methods for the analysis of functionally important residues in DNA glycosylases. Free Radic. Biol. Med 2002;32:1254–1263. [PubMed: 12057763]
12. Burgess S, Jaruga P, Dodson ML, Dizdaroglu M, Lloyd RS. Determination of active site residues in *Escherichia coli* endonuclease VIII. J. Biol. Chem 2002;277:2938–2944. [PubMed: 11711552]
13. Purmal AA, Lampman GW, Bond JP, Hatahet Z, Wallace SS. Enzymatic processing of uracil glycol, a major oxidative product of DNA cytosine. J. Biol. Chem 1998;273:10026–10035. [PubMed: 9545349]
14. Blaisdell JO, Hatahet Z, Wallace SS. A novel role for *Escherichia coli* endonuclease VIII in prevention of spontaneous G→T transversions. J. Bacteriol 1999;181:6396–6402. [PubMed: 10515930]
15. Hazra TK, Izumi T, Venkataraman R, Kow YW, Dizdaroglu M, Mitra S. Characterization of a novel 8-oxoguanine-DNA glycosylase activity in *Escherichia coli* and identification of the enzyme as endonuclease VIII. J. Biol. Chem 2000;275:27762–27767. [PubMed: 10862773]
16. Wiederholt CJ, Patro JN, Jiang YL, Haraguchi K, Greenberg MM. Excision of formamidopyrimidine lesions by endonucleases III and VIII is not a major DNA repair pathway in *Escherichia coli*. Nucleic Acids Res 2005;33:3331–3338. [PubMed: 15944451]
17. Terato H, Masaoka A, Asagoshi K, Honsho A, Ohyama Y, Suzuki T, Yamada M, Makino K, Yamamoto K, Ide H. Novel repair activities of AlkA (3-methyladenine DNA glycosylase II) and endonuclease VIII for xanthine and oxanine, guanine lesions induced by nitric oxide and nitrous acid. Nucleic Acids Res 2002;30:4975–4984. [PubMed: 12434002]

18. Zharkov, DO. Predicting functional residues in DNA glycosylases by analysis of structure and conservation. In: Bujnicki, JN., editor. Practical Bioinformatics. Springer-Verlag; 2004. p. 243-261.
19. Zaika EI, Perlow RA, Matz E, Broyde S, Gilboa R, Grollman AP, Zharkov DO. Substrate discrimination by formamidopyrimidine-DNA glycosylase: A mutational analysis. J. Biol. Chem 2004;279:4849–4861. [PubMed: 14607836]
20. Bodepudi V, Shibutani S, Johnson F. Synthesis of 2′-deoxy-7,8-dihydro-8-oxoguanosine and 2′-deoxy-7,8-dihydro-8-oxoadenosine and their incorporation into oligomeric DNA. Chem. Res. Toxicol 1992;5:608–617. [PubMed: 1445999]
21. Zharkov DO, Rosenquist TA, Gerchman SE, Grollman AP. Substrate specificity and reaction mechanism of murine 8-oxoguanine-DNA glycosylase. J. Biol. Chem 2000;275:28607–28617. [PubMed: 10884383]
22. McTigue MM, Rieger RA, Rosenquist TA, Iden CR, de los Santos CR. Stereoselective excision of thymine glycol lesions by mammalian cell extracts. DNA Repair 2004;3:313–322. [PubMed: 15177046]
23. Rieger RA, McTigue MM, Kycia JH, Gerchman SE, Grollman AP, Iden CR. Characterization of a cross-linked DNA-endonuclease VIII repair complex by electrospray ionization mass spectrometry. J. Am. Soc. Mass Spectrom 2000;11:505–515. [PubMed: 10833024]
24. Sambrook, J.; Russell, DW. Molecular Cloning: A Laboratory Manual. 3rd ed.. Cold Spring Harbor Laboratory Press; Cold Spring Harbor, NY: 2001.
25. Kraut DA, Carroll KS, Herschlag D. Challenges in enzyme mechanism and energetics. Annu. Rev. Biochem 2003;72:517–571. [PubMed: 12704087]
26. Dizdaroglu M, Laval J, Boiteux S. Substrate specificity of the *Escherichia coli* endonuclease III: Excision of thymine- and cytosine-derived lesions in DNA produced by radiation-generated free radicals. Biochemistry 1993;32:12105–12111. [PubMed: 8218289]
27. Dizdaroglu M. Application of capillary gas chromatography-mass spectrometry to chemical characterization of radiation-induced base damage of DNA: implications for assessing DNA repair processes. Anal. Biochem 1985;144:593–603. [PubMed: 3993919]
28. Miller H, Fernandes AS, Zaika E, McTigue MM, Torres MC, Wente M, Iden CR, Grollman AP. Stereoselective excision of thymine glycol from oxidatively damaged DNA. Nucleic Acids Res 2004;32:338–345. [PubMed: 14726482]
29. Stivers JT, Jiang YL. A mechanistic perspective on the chemistry of DNA repair glycosylases. Chem. Rev 2003;103:2729–2760. [PubMed: 12848584]
30. Minetti CASA, Remeta DP, Zharkov DO, Plum GE, Johnson F, Grollman AP, Breslauer KJ. Energetics of lesion recognition by a DNA repair protein: Thermodynamic characterization of formamidopyrimidine-glycosylase (Fpg) interactions with damaged DNA duplexes. J. Mol. Biol 2003;328:1047–1060. [PubMed: 12729740]
31. Zharkov DO, Grollman AP. The DNA trackwalkers: Principles of lesion search and recognition by DNA glycosylases. Mutat. Res 2005;577:24–54. [PubMed: 15939442]
32. Wong I, Lundquist AJ, Bernards AS, Mosbaugh DW. Presteady-state analysis of a single catalytic turnover by *Escherichia coli* uracil-DNA glycosylase reveals a “pinch-*pull*-push” mechanism. J. Biol. Chem 2002;277:19424–19432. [PubMed: 11907039]
33. Jiang YL, Stivers JT. Mutational analysis of the base-flipping mechanism of uracil DNA glycosylase. Biochemistry 2002;41:11236–11247. [PubMed: 12220189]
34. Kuznetsov NA, Koval VV, Zharkov DO, Nevinsky GA, Douglas KT, Fedorova OS. Kinetic basis of lesion specificity and opposite-base specificity of formamidopyrimidine-DNA glycosylase. Biochemistry. submitted
35. Bruner SD, Norman DPG, Verdine GL. Structural basis for recognition and repair of the endogenous mutagen 8-oxoguanine in DNA. Nature 2000;403:859–866. [PubMed: 10706276]
36. Gilboa R, Zharkov DO, Golan G, Fernandes AS, Gerchman SE, Matz E, Kycia JH, Grollman AP, Shoham G. Structure of formamidopyrimidine-DNA glycosylase covalently complexed to DNA. J. Biol. Chem 2002;277:19811–19816. [PubMed: 11912217]
37. Fromme JC, Banerjee A, Huang SJ, Verdine GL. Structural basis for removal of adenine mispaired with 8-oxoguanine by MutY adenine DNA glycosylase. Nature 2004;427:652–656. [PubMed: 14961129]

38. Rabow LE, Kow YW. Mechanism of action of base release by *Escherichia coli* Fpg protein: role of lysine 155 in catalysis. Biochemistry 1997;36:5084–5096. [PubMed: 9125531]
39. Rabow L, Venkataraman R, Kow YW. Mechanism of action of *Escherichia coli* formamidopyrimidine *N*-glycosylase: role of K155 in substrate binding and product release. Prog. Nucleic Acid Res. Mol. Biol 2001;68:223–234. [PubMed: 11554299]
40. Lustig MJ, Cadet J, Boorstein RJ, Teebor GW. Synthesis of the diastereomers of thymidine glycol, determination of concentrations and rates of interconversion of their *cis-trans* epimers at equilibrium and demonstration of differential alkali lability within DNA. Nucleic Acids Res 1992;20:4839–4845. [PubMed: 1408799]
41. Cathcart R, Schwiers E, Saul RL, Ames BN. Thymine glycol and thymidine glycol in human and rat urine: A possible assay for oxidative DNA damage. Proc. Natl Acad. Sci. U.S.A 1984;81:5633–5637. [PubMed: 6592579]
42. Augeri L, Lee Y-M, Barton AB, Doetsch PW. Purification, characterization, gene cloning, and expression of Saccharomyces cerevisiae redoxyendonuclease, a homolog of Escherichia coli endonuclease III. Biochemistry 1997;36:721–729. [PubMed: 9020769]
43. Venkhataraman R, Donald CD, Roy R, You HJ, Doetsch PW, Kow YW. Enzymatic processing of DNA containing tandem dihydrouracil by endonucleases III and VIII. Nucleic Acids Res 2001;29:407–414. [PubMed: 11139610]
44. Allinson SL, Dianova II, Dianov GL. DNA polymerase β is the major dRP lyase involved in repair of oxidative base lesions in DNA by mammalian cell extracts. EMBO J 2001;20:6919–6926. [PubMed: 11726527]
45. Potts RJ, Bespalov IA, Wallace SS, Melamede RJ, Hart BA. Inhibition of oxidative DNA repair in cadmium-adapted alveolar epithelial cells and the potential involvement of metallothionein. Toxicology 2001;161:25–38. [PubMed: 11295253]
46. Ischenko AA, Saparbaev MK. Alternative nucleotide incision repair pathway for oxidative DNA damage. Nature 2002;415:183–187. [PubMed: 11805838]
47. Hazra TK, Kow YW, Hatahet Z, Imhoff B, Boldogh I, Mokkapati SK, Mitra S, Izumi T. Identification and characterization of a novel human DNA glycosylase for repair of cytosine-derived lesions. J. Biol. Chem 2002;277:30417–30420. [PubMed: 12097317]
48. Fromme JC, Verdine GL. DNA lesion recognition by the bacterial repair enzyme MutM. J. Biol. Chem 2003;278:51543–51548. [PubMed: 14525999]
49. Liu J, Doetsch PW. *Escherichia coli* RNA and DNA polymerase bypass of dihydrouracil: mutagenic potential via transcription and replication. Nucleic Acids Res 1998;26:1707–1712. [PubMed: 9512542]
50. Vaisman A, Woodgate R. Unique misinsertion specificity of polι may decrease the mutagenic potential of deaminated cytosines. EMBO J 2001;20:6520–6529. [PubMed: 11707422]
51. Huffman JL, Sundheim O, Tainer JA. DNA base damage recognition and removal: New twists and grooves. Mutat. Res 2005;577:55–76. [PubMed: 15941573]
52. Vallur AC, Feller JA, Abner CW, Tran RK, Bloom LB. Effects of hydrogen bonding within a damaged base pair on the activity of wild type and DNA-intercalating mutants of human alkyladenine DNA glycosylase. J. Biol. Chem 2002;277:31673–31678. [PubMed: 12077143]
53. Chmiel NH, Livingston AL, David SS. Insight into the functional consequences of inherited variants of the hMYH adenine glycosylase associated with colorectal cancer: Complementation assays with hMYH variants and pre-steady-state kinetics of the corresponding mutated *E. coli* enzymes. J. Mol. Biol 2003;327:431–443. [PubMed: 12628248]
54. Al-Tassan N, Chmiel NH, Maynard J, Fleming N, Livingston AL, Williams GT, Hodges AK, Davies DR, David SS, Sampson JR, Cheadle JP. Inherited variants of MYH associated with somatic G:C→T:A mutations in colorectal tumors. Nat. Genet 2002;30:227–232. [PubMed: 11818965]
55. Livingston AL, Kundu S, Pozzi MH, Anderson DW, David SS. Insight into the roles of tyrosine 82 and glycine 253 in the Escherichia coli adenine glycosylase MutY. Biochemistry 2005;44:14179–14190. [PubMed: 16245934]
56. Parikh SS, Mol CD, Slupphaug G, Bharati S, Krokan HE, Tainer JA. Base excision repair initiation revealed by crystal structures and binding kinetics of human uracil-DNA glycosylase with DNA. EMBO J 1998;17:5214–5226. [PubMed: 9724657]

57. Jiang YL, Kwon K, Stivers JT. Turning on uracil-DNA glycosylase using a pyrene nucleotide switch. J. Biol. Chem 2001;276:42347–42354. [PubMed: 11551943]
58. Jiang YL, Stivers JT, Song F. Base-flipping mutations of uracil DNA glycosylase: Substrate rescue using a pyrene nucleotide wedge. Biochemistry 2002;41:11248–11254. [PubMed: 12220190]
59. Koval VV, Kuznetsov NA, Zharkov DO, Ishchenko AA, Douglas KT, Nevinsky GA, Fedorova OS. Pre-steady-state kinetics shows differences in processing of various DNA lesions by *Escherichia coli* formamidopyrimidine-DNA glycosylase. Nucleic Acids Res 2004;32:926–935. [PubMed: 14769949]
60. Fromme JC, Verdine GL. Structural insights into lesion recognition and repair by the bacterial 8-oxoguanine DNA glycosylase MutM. Nat. Struct. Biol 2002;9:544–552. [PubMed: 12055620]
61. Doublié S, Bandaru V, Bond JP, Wallace SS. The crystal structure of human endonuclease VIII-like 1 (NEIL1) reveals a zincless finger motif required for glycosylase activity. Proc. Natl Acad. Sci. U.S.A 2004;101:10284–10289. [PubMed: 15232006]
62. O'Connor TR, Graves RJ, de Murcia G, Castaing B, Laval J. Fpg protein of *Escherichia coli* is a zinc finger protein whose cysteine residues have a structural and/or functional role. J. Biol. Chem 1993;268:9063–9070. [PubMed: 8473347]
63. Tchou J, Michaels ML, Miller JH, Grollman AP. Function of the zinc finger in *Escherichia coli* Fpg protein. J. Biol. Chem 1993;268:26738–26744. [PubMed: 8253809]
64. Buchko GW, Hess NJ, Bandaru V, Wallace SS, Kennedy MA. Spectroscopic studies of zinc(II)- and cobalt(II)-associated *Escherichia coli* formamidopyrimidine-DNA glycosylase: extended X-ray absorption fine structure evidence for a metal-binding domain. Biochemistry 2000;39:12441–12449. [PubMed: 11015225]
65. Thompson JD, Higgins DG, Gibson TJ. CLUSTAL W: improving the sensitivity of progressive multiple sequence alignment through sequence weighting, position-specific gap penalties and weight matrix choice. Nucleic Acids Res 1994;22:4673–4680. [PubMed: 7984417]

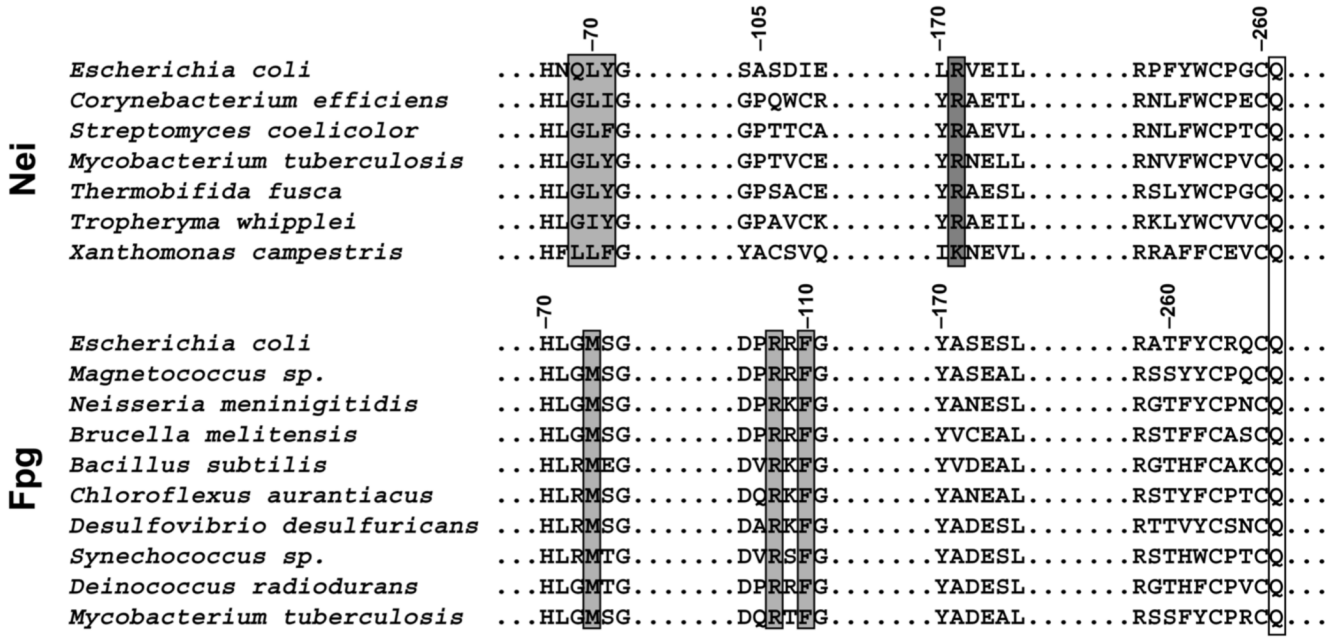

Fig. 1. Alignment of the sequences of Nei and Fpg proteins from different bacterial species

Protein sequences of Nei (top panel) and Fpg (bottom panel) were aligned using ClustalW (65). The light grey boxes indicate the intercalating residues inserted in the DNA helix; the dark grey box indicates the Arg residue conserved in Nei but not in Fpg (Arg-173 in *E. coli* Nei); the white box indicates the absolutely conserved Gln residue. Numeration of the residues in both Nei and Fpg is given according to the *E. coli* sequences.

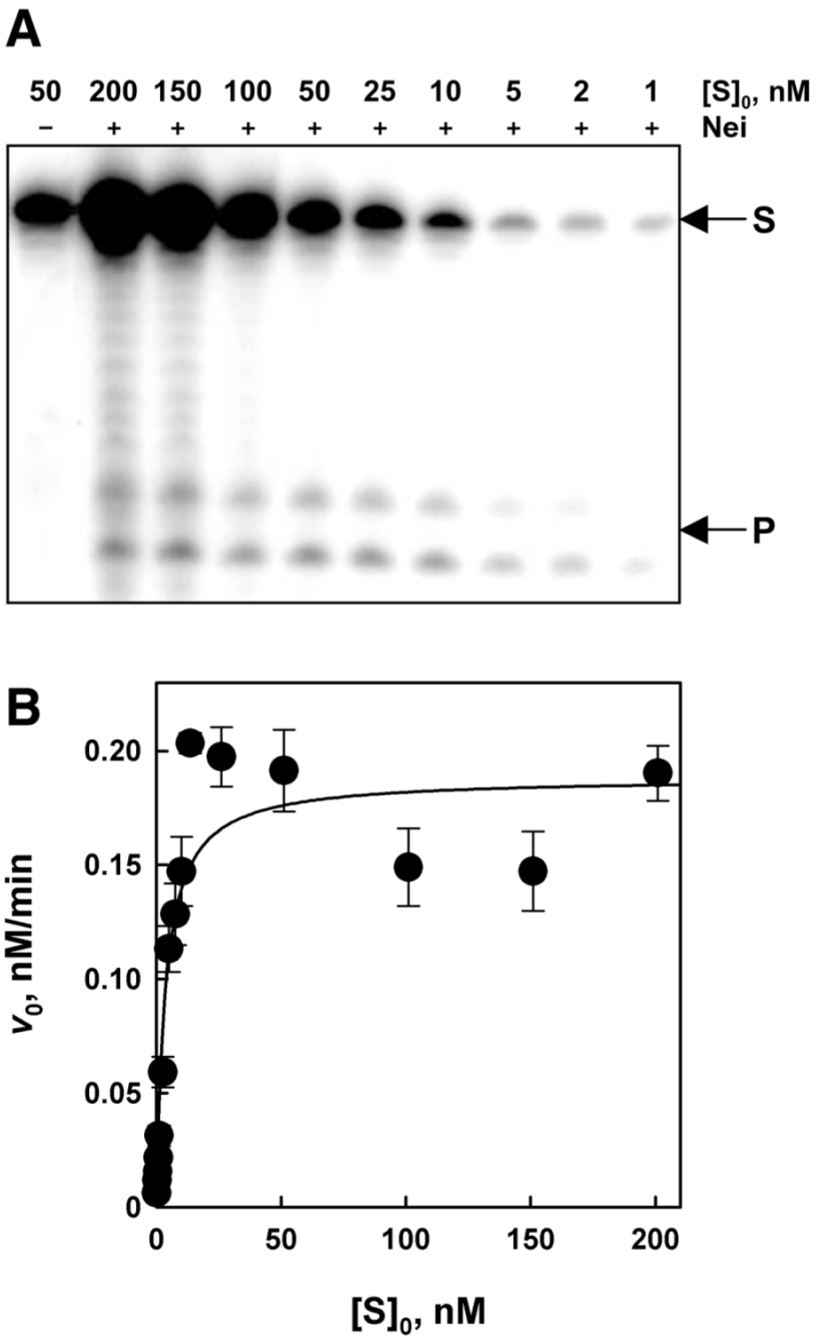

Fig. 2. Cleavage of a DHU:T substrate by wild-type Nei

(A), A gel of a representative experiment is shown. S, substrate oligodeoxyribonucleotide; P, products (Nei releases products of both β- and δ-elimination, visible as the lower-mobility and the higher-mobility species, respectively, in the product doublet band). **(B)**, The reaction velocity vs substrate concentration was plotted (3-4 experiments for each concentration, mean ± s.e.m. shown) and fit with a rectangular hyperbola to obtain the kinetic values listed in Table 2.

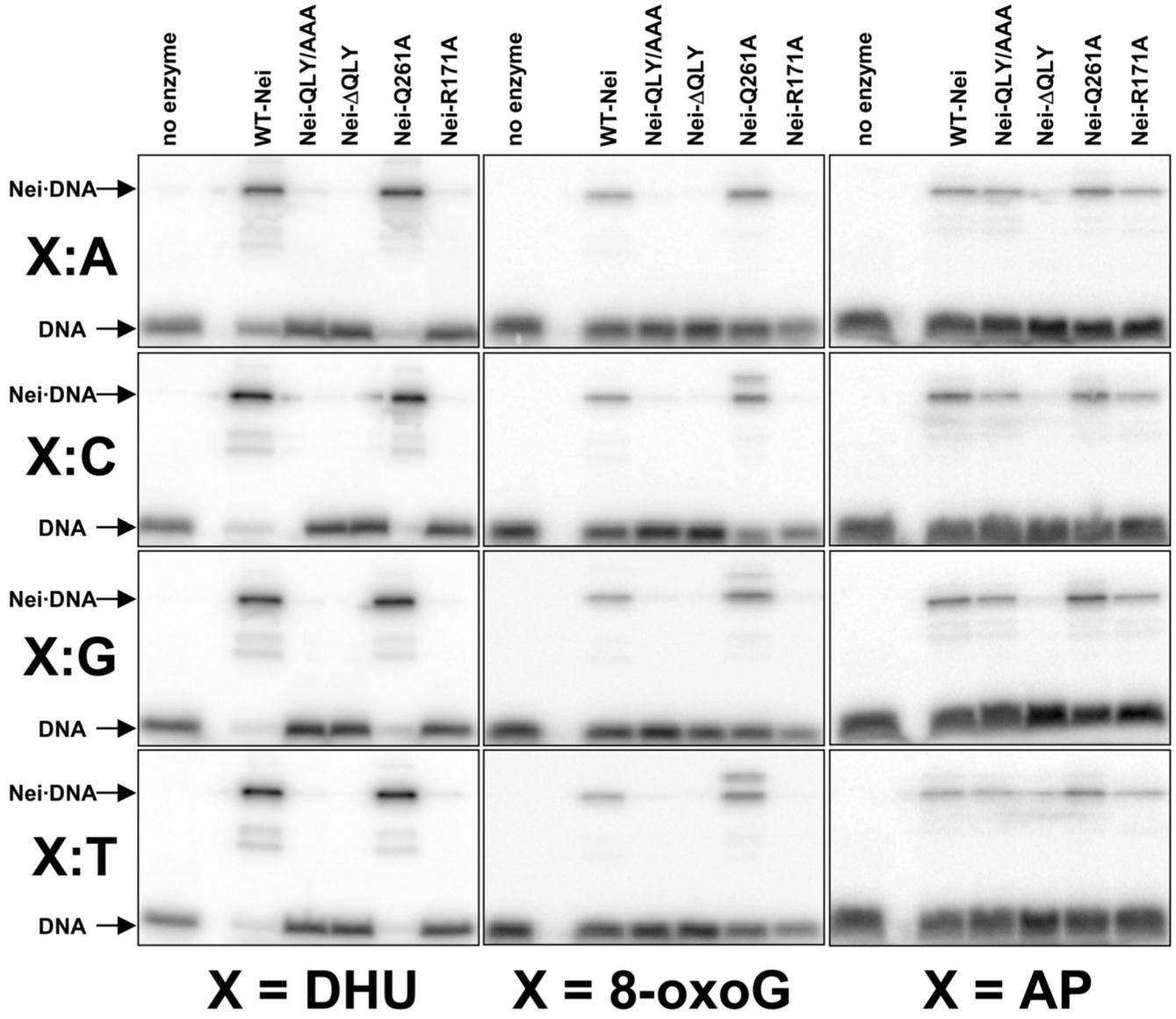

Fig. 3. Borohydride trapping of Nei and its mutants

Representative gels for wild-type Nei and Nei mutants are shown for DHU (left column), 8-oxoG (central column) and AP site (right column) opposite all bases. Arrows indicate the cross-link (Nei·DNA) and free oligonucleotides (DNA). The time of incubation was 5 min; the reactions were performed at 37°C as described in Materials and Methods.

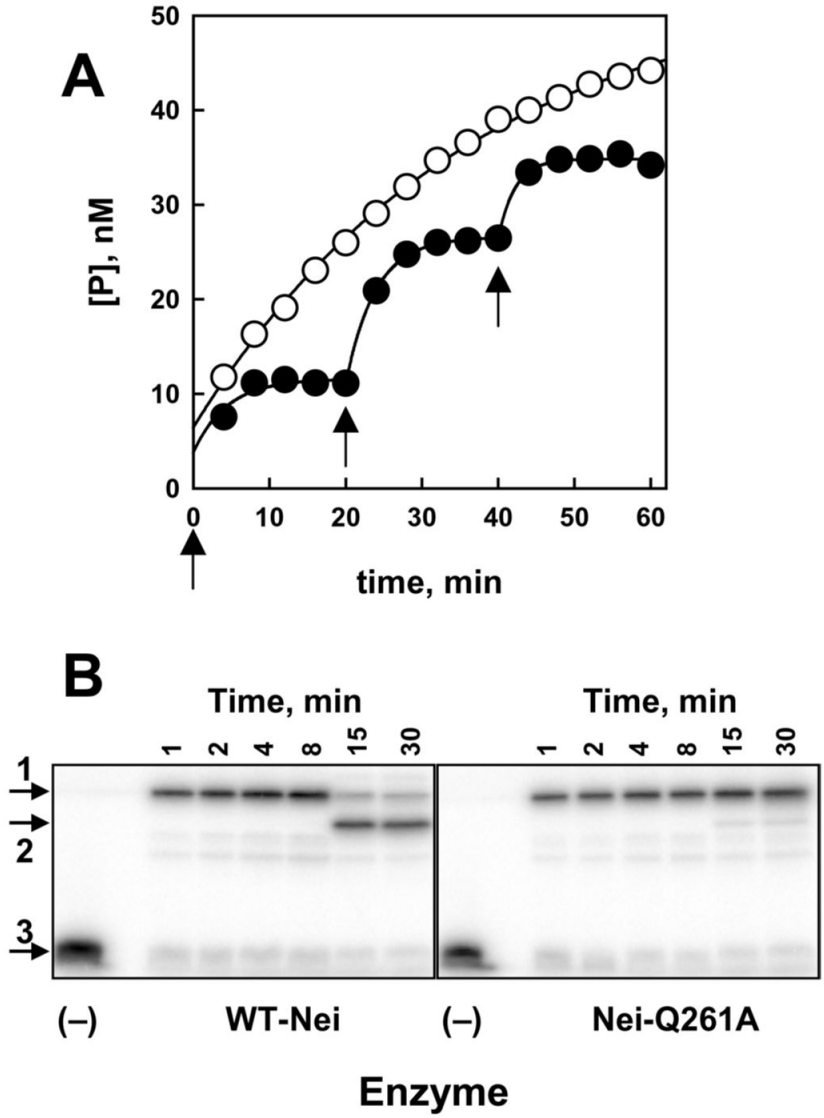

Fig. 4. Dead-end complex formation in the Nei-Q261A mutant

(A), A representative time course of product accumulation during cleavage of DHU:G (50 nM) with wild-type Nei (open circles) and Nei-Q261A (filled circles). The concentration of the enzymes was 10 nM. Arrows indicate additions of incremental 10 nM Nei-Q261A. Solid lines show a fit of the experimental data to a model with an initial burst followed by an exponential increase to a maximum. **(B)**, Time course of accumulation of cross-linked products from DHU:G by wild-type Nei and Nei-Q261A. (-), no enzyme added. Arrows correspond to the full-length cross-linking product (1), cleaved cross-linked product (2) and free oligonucleotides (3); incubation time is indicated on the figure.

Table 1

Dissociation constants (nM) of Nei and its mutants bound to DNA containing F, TgA and TgC

Lesion	Opposite base	wild-type Nei	Nei-QLY/AAA	Nei-ΔQLY	Nei-R171A	Nei-Q261A
F	A	0.47±0.11	26±7	1500±260	N/D*	N/D
	C	0.21±0.09	23±5	710±80	N/D	N/D
	G	0.29±0.12	30±6	82±35	140±110	34±8
	T	0.27±0.14	20±5	750±90	N/D	N/D
TgA	A	0.57±0.15	4.2±1.9	140±30	39±13	2.8±1.5
	C	0.93±0.34	5.5±1.6	130±30	22±4	5.5±2.5
	G	0.77±0.19	6.3±2.2	120±40	19±7	7.1±1.7
	T	0.71±0.17	3.6±1.3	180±50	14±3	21±9
TgC	A	1.6±0.4	4.5±1.9	56±12	14±3	8.1±2.5
	C	0.78±0.23	4.3±1.0	96±28	26±3	9.0±3.7
	G	1.6±0.4	4.3±0.9	75±24	15±3	11±2
	T	0.86±0.28	3.5±1.3	160±40	15±3	12±4

*N/D, not determined

Table 2

Kinetic constants of Nei and its mutants acting on different lesions

Lesion	Opposite base	wild-type Nei			Nei-QLY/AAA				Nei-ΔQLY				Nei-R171A			Nei-Q261A			
		K_M, nM	k_{cat}, min^{-1}	k_{cat}/K_M, $nM^{-1}\cdot min^{-1}$, $\times 10^3$	K_M, nM	k_{cat}, min^{-1}	k_{cat}/K_M, $nM^{-1}\cdot min^{-1}$, $\times 10^3$	relative activity[1]	K_M, nM	k_{cat}, min^{-1}	k_{cat}/K_M, $nM^{-1}\cdot min^{-1}$, $\times 10^3$	relative activity	k_{cat}/K_M, $nM^{-1}\cdot min^{-1}$, $\times 10^3$	relative activity	K_M, nM	k_{cat}, min^{-1}	k_{cat}/K_M, $nM^{-1}\cdot min^{-1}$, $\times 10^3$	relative activity
DHU	A	160± 120	0.035± 0.015	0.22	38± 21	0.0043± 0.0011	0.11	5.0×10^{-1}				UDL[2]	UDL		260± 140	0.014± 0.002	0.054	2.5×10^{-1}
	C	6.6± 2.5	0.49± 0.05	74	140± 60	0.80± 0.11	5.7	7.7×10^{-2}				UDL	UDL		270± 130	0.008± 0.001	0.030	4.1×10^{-4}
	G	8.5± 3.2	4.3± 0.5	510	42± 17	0.0039± 0.0003	0.093	1.8×10^{-4}	54± 28	0.0029± 0.0004	0.054	$1.1\times 10^{-}$	UDL		77± 73	0.009± 0.001	0.12	2.4×10^{-4}
	T	3.5± 1.3	0.19± 0.02	54	160± 120	0.70± 0.23	4.4	8.1×10^{-2}				UDL	UDL		1400± 800	0.004± 0.001	0.0029	5.4×10^{-5}
TgA	A	16± 14	1.4± 0.7	88			5.9	6.7×10^{-2}			3.7	$4.2\times 10^{-}$	2.6×10^{-3}	2.7×10^{-5}			0.18	2.0×10^{-3}
	C	4.7± 2.9	0.69± 0.18	150			5.6	3.7×10^{-2}			3.7	$2.5\times 10^{-}$	1.7×10^{-3}	1.1×10^{-5}			0.19	1.3×10^{-3}
	G	2.3± 1.2	3.4± 0.6	1500			5.4	3.6×10^{-3}			3.7	$2.5\times 10^{-}$	2.1×10^{-3}	1.4×10^{-6}	210± 100	0.34± 0.06	1.6	1.1×10^{-3}
	T	4.6± 2.6	0.67± 0.16	150			5.4	3.6×10^{-2}			3.7	$2.5\times 10^{-}$	3.0×10^{-3}	2.0×10^{-5}			0.20	1.3×10^{-3}
TgC	A	3.2± 1.6	2.1± 0.5	660			4.7	7.1×10^{-3}	66± 14	0.15± 0.01	2.3	$3.5\times 10^{-}$	5.1×10^{-3}	7.7×10^{-6}			0.18	2.7×10^{-4}
	C	4.4± 2.7	2.5± 0.8	570			5.5	9.6×10^{-3}			2.9	$5.1\times 10^{-}$	2.8×10^{-3}	4.9×10^{-6}			0.17	3.0×10^{-4}
	G	2.3± 0.8	2.0± 0.3	870	49± 37	0.96± 0.21	20	2.3×10^{-2}			3.1	$3.6\times 10^{-}$	4.4×10^{-3}	5.1×10^{-6}	240± 120	0.35± 0.07	1.5	1.7×10^{-3}
	T	4.4± 1.6	2.9± 0.6	660	190± 80	1.3± 0.2	6.8	1.0×10^{-2}			2.8	$4.2\times 10^{-}$	5.3×10^{-3}	8.0×10^{-6}			0.17	2.6×10^{-4}
8-oxoG	A	610± 110	0.47± 0.04	0.78			4.6×10^{-3}	5.9×10^{-3}				UDL	3.7×10^{-3}	4.7×10^{-3}			2.0×10^{-5}	2.6×10^{-5}
	C	680± 210	0.95± 0.10	1.4			6.6×10^{-3}	4.7×10^{-3}				UDL	1.1×10^{-3}	7.9×10^{-4}			4.3×10^{-5}	3.1×10^{-5}
	G	580± 200	0.79± 0.11	1.4			5.8×10^{-3}	4.1×10^{-3}				UDL	1.7×10^{-3}	1.2×10^{-3}			3.8×10^{-5}	2.7×10^{-5}
	T	1300± 300	1.4± 0.2	1.1			5.5×10^{-3}	5.0×10^{-3}				UDL	2.9×10^{-3}	2.6×10^{-3}			1.4×10^{-5}	1.3×10^{-5}
AP	A	0.083± 0.015	0.64± 0.02	7700	28± 7	0.09± 0.01	3.2	4.2×10^{-4}				UDL	1×10^{-3}	1.3×10^{-7}				UDL
	G	0.11± 0.03	0.53± 0.13	4800	22± 3	0.11± 0.02	5.0	1.0×10^{-3}				UDL	6×10^{-4}	1.3×10^{-7}				UDL

[1] Relative activity defined as the ratio of the specificity constant (k_{cat}/KM) for the mutant to that for the wild-type enzyme.

[2] UDL, under detection limit.